Journal of Alloys and Compounds 502 (2010) 289–294

Contents lists available at ScienceDirect

Journal of Alloys and Compounds

journal homepage: www.elsevier.com/locate/jallcom

Low temperature hydrothermal synthesis of N-doped TiO_2 photocatalyst with high visible-light activity

Deyong Wu [a], Mingce Long [a,*], Weimin Cai [a,*], Chao Chen [b], Yahui Wu [b]

[a] School of Environmental Science and Engineering, Shanghai Jiao Tong University, Dong Chuan Road 800, Shanghai 200240, China
[b] Department of Environmental Science and Engineering, School of Civil and Environmental Engineering, Harbin Institute of Technology, Harbin 150090, China

ARTICLE INFO

Article history:
Received 14 January 2010
Received in revised form 20 April 2010
Accepted 25 April 2010
Available online 5 May 2010

Keywords:
Photocatalysis
Titanium dioxide
Nitrogen doping
Photodecomposition

ABSTRACT

A visible-light-active TiO_2 photocatalyst was prepared through nitrogen doping, employing triethylamine as nitrogen source, by a low temperature hydrothermal method without further calcinations. The prepared samples were characterized by X-ray diffraction, transmission electron microscopy, X-ray photoelectron spectroscopy, diffuse reflectance spectra. A shift of the absorption edge to a lower energy and a stronger absorption in the visible-light region were observed in the N-TiO_2 samples. Comparing to P25 and undoped TiO_2, greatly improved photocatalytic activity, decomposing methyl orange dye solutions under visible-light irradiation, was obtained as a result of the doping of nitrogen into the titania system, that was evidenced by the formation of O–Ti–N bonds. In addition, the photocatalytic activity of N-TiO_2 was strongly affected by the hydrothermal temperature and pH value in the process of preparing the samples.

1. Introduction

Semiconductor photocatalysts have attracted much attention because of their potential application in the removal of recalcitrant organic pollutants in air or water [1–3]. Especially, titanium dioxide (TiO_2), as a cheap, nontoxic, and highly efficient photocatalyst, has been widely investigated in many areas [4–6]. However, owing to its wide band gap (3.2 eV for anatase), TiO_2 can only be excited under ultraviolet irradiation, which occupies only about 3–5% of the total solar irradiance at the Earth's surface. For the sake of efficient utilization of sunlight, which contains visible-light up to 45–50%, many routes have been developed to synthesize modified TiO_2 with visible-light responsive activity [7–9].

Substitutional or interstitial doping of non-metallic elements, such as C [7,10,11], N [12–14], S [15], I [16–18] and P [19,20], seems to be a very promising way to efficiently extend the optical response of TiO_2 from ultraviolet to visible-light region. Especially, the synthesis of N-doped TiO_2 (N-TiO_2) has been the focus of recent photocatalyst researches. Various strategies have been achieved, either based on physical methods (mechanical milling [21], magnetron sputtering [22], etc.) or based on chemical reactivity (sol–gel synthesis [23], oxidation of titanium nitride [24], etc.), to incorporate nitrogen into titanium dioxide. However, physical methods usually need expensive apparatus [21,22], and chemical methods always involve a high temperature treatment process in the preparation method (often >300 °C) [24,25].

From the perspective of energy saving, it is obvious that formation of N-TiO_2 photocatalysts at low temperature is of great significance. Moreover, the formation of N-TiO_2 photocatalysts at low temperature is important for the fabrication of films on substrates which cannot sustain high temperature treatment, such as plastics, textiles and wood-based materials. Gole et al. have reported that N-TiO_2 photocatalyst can be prepared at room temperature through treating TiO_2 nano-sol with triethylamine (TEA) with a large amount of palladium salt [26]. However, Han and Bai confirmed that the TiO_2 nano-sol cannot be turned into crystallined TiO_2 photocatalyst after TEA treatment without using the expensive precious metal salt as the phase transfer catalyst [27]. Meanwhile, they have successfully developed a method to prepare N-TiO_2 photocatalyst from an ethanol-based sol by refluxing TiO_2 nano-sol with TEA in the presence of acetyl acetone (AcAc) [27]. Whereas, for making the whole chemical approach environmentally friendly, the utilization of aqueous solutions instead of organic solvents is desirable in the practical application. In the present paper, we successfully prepared N-TiO_2 particles from a water-based TiO_2 sol hydrothermally treated with TEA at low temperature. It was found to be a simple and effective way to obtain N-TiO_2 nanoparticles with excellent degradation of methyl orange under visible-light. Using water-based TiO_2 sol as precursor, which was then treated with triethylamine at room temperature and subsequently heated in the hydrothermal process at low temperature, we could combine nitrogen doping and transformation of amor-

* Corresponding authors. Tel.: +86 21 54747354; fax: +86 21 54748019.
E-mail addresses: long_mc@sjtu.edu.cn (M. Long), wmcai@sjtu.edu.cn (W. Cai).

0925-8388/$ – see front matter © 2010 Elsevier B.V. All rights reserved.
doi:10.1016/j.jallcom.2010.04.189

phous titania to nanocrystalline into one simple process. The results indicated that N-TiO_2 nanoparticles synthesized in the way showed a considerably enhanced activity of visible-light-induced photodecomposition of organic pollutants.

2. Experimental

2.1. Material preparation

Firstly, a TiO_2 nano-sol was prepared according to the following typical steps: under the stirring at room temperature, a mixture of 5 ml of titanium *n*-butoxide ($Ti(OBu)_4$, CP, Sinopharm) and 5 ml of isopropyl alcohol was added dropwise into 30 ml HNO_3 solution (0.2 mol/L) containing 1 ml of acetyl acetone (AcAc, CP, Sinopharm). Then, the mixture was aged overnight with stirring for 12 h to obtain a transparent nano-sol. Subsequently, the TiO_2 nano-sol was treated with triethylamine (TEA, 99%, Sinopharm) for 12 h by adding 5.0 ml of TEA into the sol with stirring at ambient temperature. The initial pH of the mixture was 10.02, and a lower desired pH could be adjusted by HNO_3 solution (5 mol/L). Then, the mixture was poured into a Teflon-lined stainless autoclave (50 ml), and hydrothermally treated at desired temperature for 12 h. The temperature was 160 °C in most cases but also varied with different temperatures (120 °C, 140 °C) in other experiments. The reaction products were filtered, washed with deionized water five times, and dried in air at 70 °C. Fine N-TiO_2 powders were obtained eventually. To consider the effect of TEA and AcAc on the properties of nanocatalysts, samples were prepared in the same process but without adding TEA or AcAc. We designated the three different samples as TiO_2-A (TEA-treated TiO_2 powder in the absence of AcAc), TiO_2 (TiO_2 powder in the presence of AcAc but without TEA treatment) and N-TiO_2 (TEA-treated TiO_2 powder in the presence of AcAc).

2.2. Material characterization

The nanometric structure and the morphology of the catalyst powders were observed by Transmission Electron Microscope (TEM, JEM-100CX, JEOL, Japan). The crystal phase and crystallinity of samples were characterized by powder X-ray diffraction (XRD, D/max-2200/PC, Rigaku Corporation, Japan) with Cu K_a radiation, operating at 40 kV and 30 mA, where $\lambda = 0.15418$ nm for the Cu K_a line. A diffuse reflectance UV–vis spectrophotometer (DRS, TU-1901) was used to obtain the optical absorption spectra of samples. The elemental analysis was carried out on an Elementar Vario EL III. XPS experiments were carried out on a RBD upgraded PHI-5000C ESCA system (Perkin Elmer, USA), the shift of the binding energy due to relative surface charging was corrected using the C 1s level at 284.6 eV as an internal standard.

2.3. Photocatalytic activity measurements

The photocatalytic activity was evaluated by measuring the decomposition of the methyl orange (MO) solution with a concentration of 10 mg/L. A 1000 W xenon lamp was used as the light source of the homemade photoreactor, surrounded with a water circulation facility at the outer wall through a quartz jacket. The short wavelength components ($\lambda < 400$ nm) of the light were cut off using a glass optical filter. The distance between the lamp and the center of the beaker was 100 cm. For a typical photocatalytic experiment, a total of 0.05 g of catalyst powders was added to 50 ml of the above methyl orange solution in the beaker with stirring. Prior to irradiation, the suspensions were magnetically stirred in the dark for 30 min to ensure the establishment of an adsorption/desorption equilibrium. Samples were taken out at regular time intervals. The concentration of MO was monitored at 464 nm by spectrophotometry with a UNICO 7200 Spectrophotometer.

3. Results and discussion

3.1. Characterization of photocatalysts

The morphologies of TiO_2 and N-TiO_2 are clearly displayed on their TEM images in Fig. 1. The rod shape structure can be observed for TiO_2. It is a reason of the AcAc as an inhibiting agent to coordinate the Ti center. A similar morphology can be obtained by different inhibiting agents and controllable sol–gel parameters [28,29]. The particle size of TiO_2 was not uniform; and particles with a dimension from around 1 nm × 2 nm to 6 nm × 10 nm can be found (Fig. 1a). However, the shape of N-TiO_2 was clearly different from that of TiO_2. N-TiO_2 particles possessed relative uniform dimension at about 5 nm. These results indicated that the TEA treatment of the TiO_2 nano-sol affected the morphologies of the photocatalyst particles. As we known, the sol–gel process of titanium oxide polymer formation consists of hydrolysis and polycondensation, and the later one included both deprotonation and dehydroxylation polycondensation. TEA can be served not only as a ligand coordination to titanium for inhibiting the hydrolysis but also as a base catalyst to promote the deprotonation polycondensation [29]. Therefore the sol–gel process carries out more gently to ensure more uniform nanoparticles.

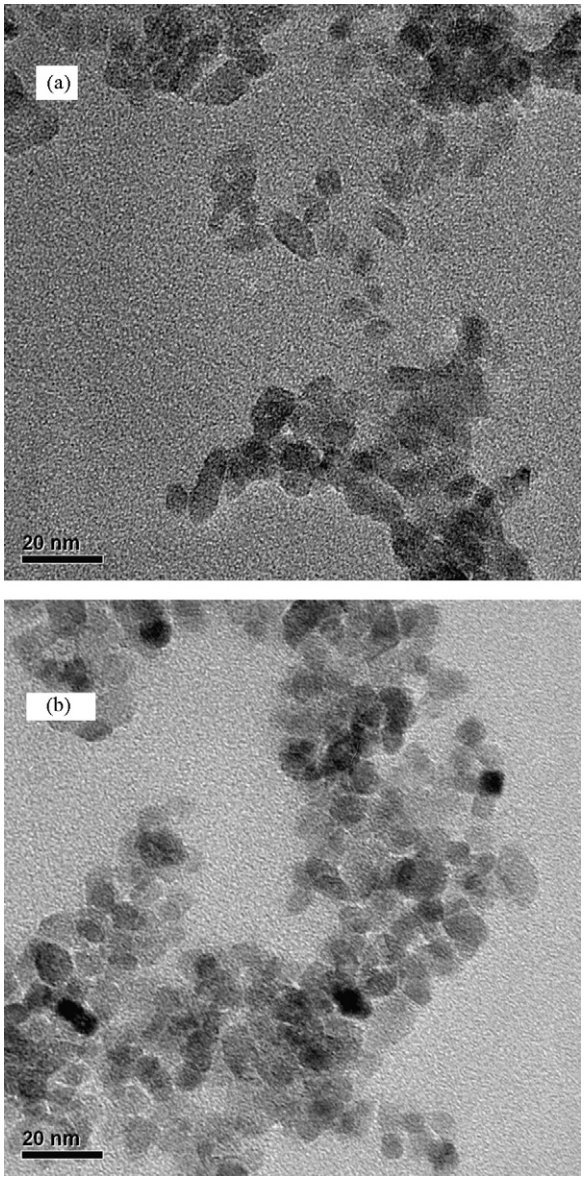

Fig. 1. HR-TEM images: (a) TiO_2 and (b) N-TiO_2.

The XRD patterns for the three samples are shown in Fig. 2. The presence of exclusive anatase phase of titanium dioxide can be observed (JCPDS, No. 21-1272) in all of these samples. Observed from the XRD results, the TEA treatment on the TiO_2 sol seem to not affect the crystal structure. According to Scherrer's equation, $L_c = K\lambda/(\beta \cos\theta)$ [30] (where λ is the X-ray wavelength, β is the FWHM of the diffraction line, θ is the diffraction angle, and K is a constant, which has been assumed to be 0.9), and based on the full width at half maximum (FWHM) of the (1 0 1) peak, an average particle diameter of about 6.3 nm and 4.1 nm for TiO_2 and N-TiO_2, respectively, can be calculated, which was strongly consistent with the observation from TEM (Fig. 1). In addition, the lattice distortion has been calculated by the following equation: $\varepsilon = n_{hkl}/(4 \operatorname{tg}\theta)$ (n_{hkl} is the FWHM of the diffraction line, θ is the diffraction angle).

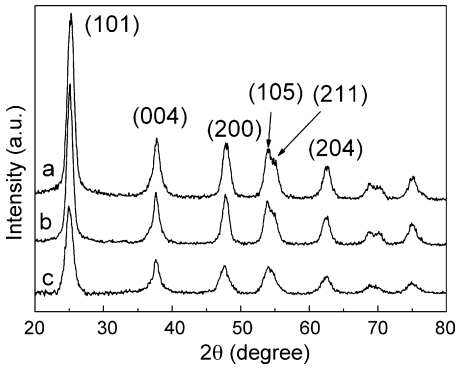

Fig. 2. XRD patterns: (a) N-TiO_2, (b) TiO_2 and (c) TiO_2-A.

The lattice distortions were 0.025 and 0.038 for TiO_2 and N-TiO_2, respectively. The slight bigger lattice distortion after N doping indicates the presence of the nitrogen in the TiO_2 lattice sites.

Fig. 3 shows the UV–vis absorption spectra for TiO_2-A, TiO_2 and N-TiO_2. It was obvious that N-TiO_2 powers exhibit significantly more absorption in the visible-light range than the other two samples, and the absorption edge was, in fact, even up to 800 nm against the light wavelength. Assuming the N-TiO_2 to be indirect semiconductor, as is TiO_2, for which the relation between absorption coefficient (a) and the incident photon energy ($h\nu$) can be written as $a = B_i(h\nu - E_g)^2/h\nu$, where B_i is the absorption constant for indirect transitions [31], a plot of $(ah\nu)^{1/2}$ versus $h\nu$ affords the band gap energy as shown in Fig. 3. The band gaps optically obtained in such a way were approximately 3.3, 3.15 and 2.76 eV for TiO_2-A, TiO_2 and N-TiO_2, respectively. The above results suggested that the nitrogen doping was the synergistic effect of AcAc and TEA. It is necessary to employ AcAc to inhibit the initial hydrolysis of titanium alkoxyl and TEA to coordinate the metallic Ti center, accompanying with hydrothermal reaction to promote the nitrogen doping taking place.

3.2. Photocatalytic activities

The photocatalytic activities of the prepared samples were measured on the degradation of MO in water under visible-light irradiation. Fig. 4 represents the variation of MO concentration (C/C_0) with irradiation time over different catalysts under visible-light irradiation. As a comparison, photocatalysis of MO over P25 was also performed under identical conditions. Although, all the degradation ratios of MO on the prepared samples were higher than that on the well-known photocatalyst P25, which only degraded about 3% of MO. TiO_2 and TiO_2-A only could degrade 8% and 11% of MO in 120 min under visible-light irradiation, respectively. Interestingly, MO can be effectively degraded in the presence of N-TiO_2, and the degradation efficiency reached about 80% in 120 min. The apparent rate constant (k) has been chosen as the basic kinetic parameter for the different photocatalysts, which was fitted by the equation $\ln(C/C_0) = -kt$, where k is apparent rate constant, C is the solution-phase concentration of organic pollutant (in this case, MO), and C_0 is the initial concentration of MO [32]. The apparent rate constant of N-TiO_2 and TiO_2 was 0.0135 min^{-1}, and 6.95×10^{-4} min^{-1}, respectively. The photocatalytic efficiency of N-TiO_2 under visible-light irradiation is estimated to be about 19 times higher than that of TiO_2. The stronger absorption of N-TiO_2 in the visible-light region, as shown in Fig. 3, must be an important reason. Nitrogen doping would result in narrowing the banding energy of the sample, therefore N-TiO_2 can be excited under visible-light irradiation [33], resulting in the formation of reactive oxygen species, which can break down MO to smaller fragments that eventually decomposed into simple inorganic minerals.

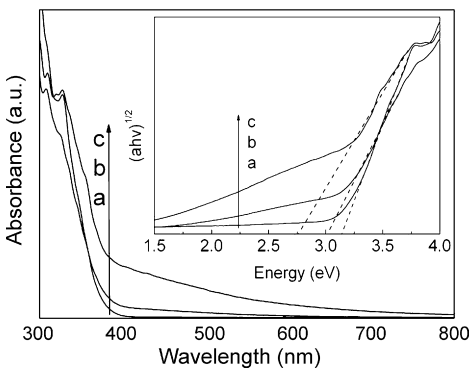

Fig. 3. UV–vis absorption spectra: (a) TiO_2-A, (b) TiO_2 and (c) N-TiO_2. The inset was the estimated band gap by Kubelka–Munk function.

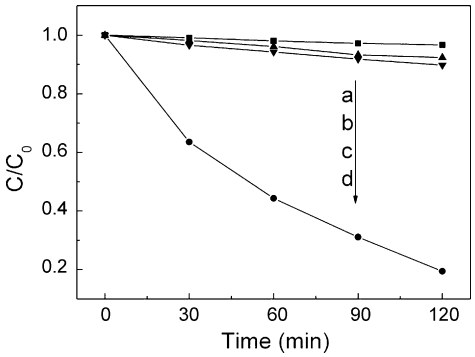

Fig. 4. Photocatalytic activity for decolorization of MO dye solutions under visible-light irradiation by the photocatalyst respectively: (a) P25, (b) TiO_2, (c) TiO_2-A and (d) N-TiO_2 powder samples.

3.3. Chemical states of the doped nitrogen

Because the N-TiO_2 showed stronger absorption in the visible-light region (Fig. 3) and higher photocatalytic decomposition efficiency (Fig. 4), thereafter, we further investigated chemical states of the doped nitrogen by XPS. Although there are much work on the nitrogen doped TiO_2, the diverse chemical states of doping nitrogen species from different synthesis methods are still in disputations [34,35]. It could be seen from Fig. 5a that two N 1s peaks were found at 396.2 eV and around 399.5 eV. The binding energy at 396.2 eV, which can be attributed to nitrogen replacing the oxygen in the crystal lattice of TiO_2 [36,37], was confirmed in various N-TiO_2 samples from previous reports [36–38]. It indicates that Ti–N binding was actually formed in the lattice of the titania crystal during the hydrothermal treatment. After fitting the peak at around 399.5 eV, two peaks were obtained at 399.1 and 399.7 eV, respectively. We attribute the peak at 399.1 eV to the N^- anion incorporated in the TiO_2 as N–Ti–O structural feature, which is consistent with the present characteristics of other literatures [38–40]. Because of the high electronegativity of oxygen, leading to the reducing of electron density on the nitrogen, a relatively higher binding energy at 399.1 eV observed compared to Ti–N. This was also further supported by the results of XPS spectra for the Ti 2p region (Fig. 5b). The Ti $2p_{3/2}$ and Ti $2p_{1/2}$ core levels of the N-TiO_2 appear at 458.2 and 463.9 eV, respectively. According to the XPS standard spectrum, the Ti $2p_{2/3}$ peak of TiO_2 should be at 458.8 eV [41]. The decreases of the binding energy of Ti $2p_{3/2}$ after nitrogen doping showed that the electronic interaction of Ti with anions is considerably different from that of TiO_2. On account of the lower electronegativity of nitrogen compared to oxygen, partial electron

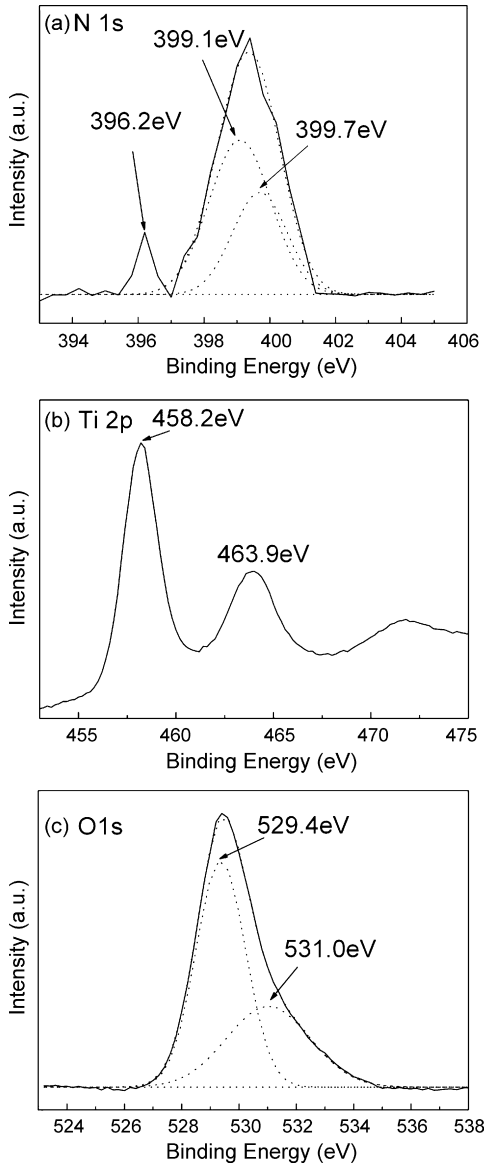

Fig. 5. X-ray photoelectron spectra of N-TiO_2 samples: (a) N 1s, (b) Ti 2p and (c) O 1s.

can transfer from the N to the Ti. As a result, the electron density around the anion decreases, resulting in the increase in electron density around the cation [39]. This further testified that nitrogen incorporates into the lattice and substitutes for oxygen. And the binding energy at 399.7 eV signified that the nitrogen was in the Ti–O–N site in the N-TiO_2 matrix [41,42]. It can be analyzed by combining the N 1s and O 1s core levels. As shown in Fig. 5c, an additional peak appeared at 531.0 eV, which was attributed to the presence of Ti–O–N bonds [38,43,44]. From the above observations, it can be concluded that the chemical states of the doped nitrogen in TiO_2 are in various forms.

3.4. Effect of the hydrothermal treatment temperature

Normally, the treatment temperature greatly affected the photoactivity of N-TiO_2 products [39,45,46]. Thus, TEA-treated TiO_2 photocatalyst was further examined for 120 °C, 140 °C, 160 °C and 180 °C of hydrothermal temperature, respectively. The visible-light driven photocatalytic activities of these powders for MO degradation have been tested. As shown in Fig. 6, the photocatalytic

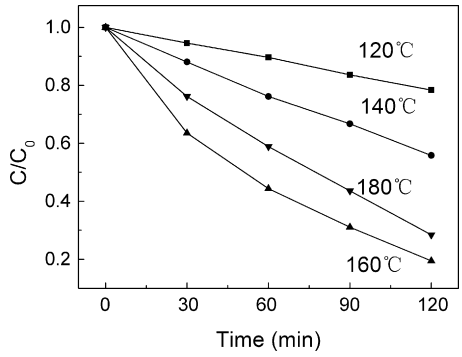

Fig. 6. MO dye decolorization rate for the prepared N-TiO_2 photocatalysts with different temperatures.

degradation percents of MO are about 22%, 45%, 80% and 72% in 120 min for N-TiO_2 samples hydrothermal treated at 120 °C, 140 °C, 160 °C and 180 °C, respectively. Their optical absorption performances are presented in Fig. 7. It was clear observed that the absorption range of the photocatalysts in the visible-light was greatly improved by increasing the treatment temperature. Especially, the photocatalyst treated at 160 °C achieved much more absorption in the visible-light compared to N-TiO_2 prepared at 120 °C and 140 °C. The results suggested that the photocatalytic properties of these samples are corresponding to their optical absorption performance. Moreover, according to elemental analysis, the nitrogen contents were about 0.09, 0.11, 0.15 at% for N-TiO_2 samples treated at 120 °C, 140 °C, 160 °C, respectively. The increase of N content was also favor for improving the photocatalytic activity under visible-light irradiation [47]. Therefore the powder treated at 160 °C exhibited better photocatalytic performance. Interestingly, the photocatalytic activity of N-TiO_2 sample treated at 180 °C was slightly less than that of the sample treated at 160 °C. Observed from Fig. 7, there was no obvious difference of the absorption range between the photocatalysts prepared at 160 °C and 180 °C. But, the nitrogen content of N-TiO_2 prepared at 180 °C was 0.13 at%, which was less than that of N-TiO_2 prepared at 160 °C. From the above, the optimal treatment temperature in our method was about 160 °C.

3.5. Effect of pH on the photocatalytic activity of N-TiO_2

It is interesting that the pH value in the preparation process greatly affected the doping nitrogen concentration and consequently on the photocatalytic activity of N-TiO_2 photocatalysts [40,48,49]. In order to investigate the effects of pH value in the process of preparing the photocatalysts on the photocatalytic activity, the pH value of the TiO_2 sol was adjusted by HNO_3 solution

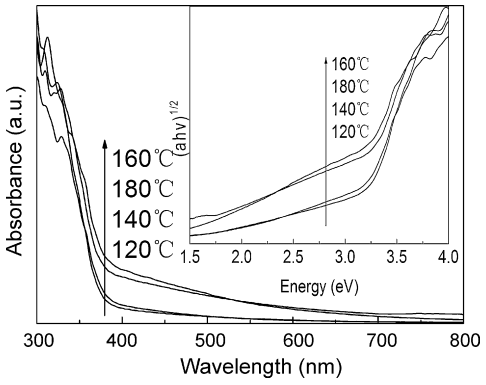

Fig. 7. UV–vis absorption spectra for the prepared photocatalyst with hydrothermal temperature for 120 °C, 140 °C, 160 °C and 180 °C, respectively.

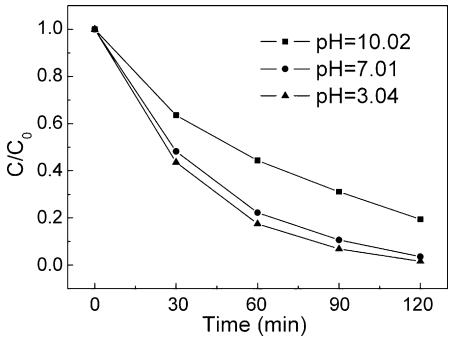

Fig. 8. Effect of pH on the photocatalytic activity of N-TiO_2.

(5 mol/L) to 7.01 or 3.04 before hydrothermal treatment. And the initial pH value of the TiO_2 sol after adding 5 ml TEA was 10.02. The samples prepared at pH 3.04, 7.01 and 10.02 were noted as N-TiO_2-3, N-TiO_2-7 and N-TiO_2-10. Observed from Fig. 8, the visible-light activity of N-TiO_2 was increased with the decrease of pH in the preparative process. From DRS (Fig. 9), there is no obvious difference in their optical absorption properties. However, significant difference of nitrogen concentration in the catalysts can be observed, and it can be regarded as the reason of the effects of pH [38,40,49]. According to elemental analysis, the nitrogen contents were about 0.93, 1.90, 0.15 at% for N-TiO_2-3, N-TiO_2-7 and N-TiO_2-10, respectively. The former two are distinctly larger than the last one, the same as their photocatalytic activity. Interestingly, the nitrogen concentration of the N-TiO_2-7 was much higher than that of N-TiO_2-3, but the visible-light activity of N-TiO_2-7 was slightly less than that of N-TiO_2-3 (Fig. 8). We suggested that this phenomenon should be attributed to the existence of optimum nitrogen dopant for N-TiO_2 [47]. At higher doping levels (C_N > 1 at%), the energy gap has hardly further narrowing compared with that at lower doping levels [50], because N was difficult to substitute for O at high nitrogen doping levels [47]. In addition, increasing the nitrogen concentration would induce more undesirable deep-level defects [47] and lower the quantum yields [51]. So the paradox can be understood according to their different nitrogen concentrations. Meanwhile, the nitrogen concentrations of N-TiO_2-3 and N-TiO_2-7 were in the range of the optimum nitrogen dopant (C_N = ~1–2 at%) [47], so small difference of their activities was reasonable. It can be understood that nitrogen concentration depends strongly on the pH values in the preparation. A similar result has been obtained by Sun et al. [49]. According to the density functional theory (DFT) calculation, formation of NH_3 in the Ti complex was regarded playing the greatest role in the nitrogen concentration in the doping process with $TiCl_4$ hydrolyzing accompanying hydrazine hydrate [49]. In our case, the processes contributed to the effect of pH on the nitrogen concentration including the TEA forms and configuration of Ti complex, zeta potential of TiO_2 sol and surface adsorption, and the hydrothermal crystallize. Anyway, lowing pH to 3 promotes the nitrogen doping and improves the nitrogen concentration in the products, so as to contribute a better visible-light photocatalytic activity.

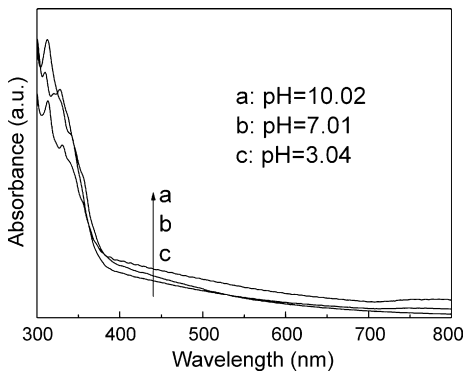

Fig. 9. UV–vis absorption spectra for the photocatalysts prepared at different pH values.

4. Conclusions

High-quality N-TiO_2 nanoparticles exhibiting visible-light photocatalysis can be synthesized at low temperature by the hydrothermal treatment. N-TiO_2 powders own significant absorbance in the visible-light range (400–700 nm), and the absorption edge is, in fact, even up to 800 nm against the light wavelength. Structural studies show that all the TiO_2-based photocatalysts have the simplex crystal structure of anatase. Transmission electron microscopy reveals that the particle size is in the range of 5–8 nm for N-TiO_2. X-ray photoelectron spectroscopy indicates that the chemical states of the nitrogen doped in TiO_2 may be various and coexist in the form of N–Ti–O and Ti–O–N. Experiments conducted for decolorization of methyl orange dye solutions show the effectiveness of the prepared novel photocatalyst under the visible-light. It was found that N-TiO_2 showed significantly higher photocatalytic activity than P25 and undoped TiO_2 on the degradation of MO under visible-light irradiation (λ > 400 nm), even though the sample was prepared at temperature as low as 120 °C. Moreover, the visible-light activity of N-TiO_2 was increased with the decrease of pH value in the preparative process. The prepared photocatalyst has the prospect to be used for photocatalytic decontamination of organic pollutants in water or used water.

Acknowledgments

We are thankful for the financial support by National Natural Science Foundation of China (20907031). We gratefully acknowledge the support in TEM measurements by Ms. Xinqiu Guo of the Instrumental Analysis Center of Shanghai Jiao Tong University.

References

[1] M.C. Long, W.M. Cai, J. Cai, B.X. Zhou, X.Y. Chai, Y.H. Wu, J. Phys. Chem. B 110 (2006) 20211–20216.
[2] S.M. Sun, W.Z. Wang, L. Zhang, L. Zhou, W.Z. Yin, M. Shang, Environ. Sci. Technol. 43 (2009) 2005–2010.
[3] X. Zhao, T.G. Xu, W.Q. Yao, C. Zhang, Y.F. Zhu, Appl. Catal. B: Environ. 72 (2007) 92–97.
[4] Q. Zheng, B.X. Zhou, J. Bai, L.H. Li, Z.J. Jin, J.L. Zhang, J.H. Li, Y.B. Liu, W.M. Cai, X.Y. Zhu, Adv. Mater. 20 (2008) 1044–1049.
[5] M.I. Mejia, J.M. Marin, G. Restrepo, C. Pulgarin, E. Mielczarski, J. Mielczarski, Y. Arroyo, J.C. Lavanchy, J. Kiwi, Appl. Catal. B: Environ. 91 (2009) 481–488.
[6] C. Euvananont, C. Junin, K. Inpor, P. Limthongkul, C. Thanachayanont, Ceram. Int. 34 (2008) 1067–1071.
[7] C. Chen, M.C. Long, W.M. Cai, B.X. Zhou, J.Y. Zhang, Y.H. Wu, D.W. Ding, D.Y. Wu, J. Mol. Catal. A: Chem. 319 (2009) 35–41.
[8] J. Zhu, J. Ren, Y.N. Huo, Z.F. Bian, H.X. Li, J. Phys. Chem. C 111 (2007) 18965–18969.
[9] H. Irie, K. Kamiya, T. Shibanuma, S. Miura, D.A. Tryk, T. Yokoyama, K. Hashimoto, J. Phys. Chem. C 113 (2009) 10761–10766.
[10] Y. Huang, W. Ho, S. Lee, L. Zhang, G. Li, J.C. Yu, Langmuir 24 (2008) 3510–3516.
[11] H. Liu, A. Imanishi, Y. Nakato, J. Phys. Chem. C 111 (2007) 8603–8610.
[12] E. Finazzi, C.D. Valentin, A. Selloni, G. Pacchioni, J. Phys. Chem. C 111 (2007) 9275–9282.
[13] H. Choi, M.G. Antoniou, M. Pelaez, A.A.D.L. Cruz, J.A. Shoemaker, D.D. Dionysiou, Environ. Sci. Technol. 41 (2007) 7530–7535.
[14] S. Livraghi, M.C. Paganini, E. Giamello, A. Selloni, C.D. Valentin, G. Pacchioni, J. Am. Chem. Soc. 128 (2006) 15666–15671.
[15] F. Tian, C. Liu, J. Phys. Chem. B 110 (2006) 17866–17871.
[16] X.T. Hong, Z.P. Wang, W.M. Cai, F. Lu, J. Zhang, Y.Z. Yang, N. Ma, Y.J. Liu, Chem. Mater. 17 (2005) 1548–1552.
[17] S. Tojo, T. Tachikawa, M. Fujitsuka, T. Majima, J. Phys. Chem. C 112 (2008) 14948–14954.
[18] G. Liu, Z.G. Chen, C.L. Dong, Y.N. Zhao, F. Li, G.Q. Lu, H.M. Cheng, J. Phys. Chem. B 110 (2006) 20823–20828.
[19] K.S. Yang, Y. Dai, B.B. Huang, J. Phys. Chem. C 111 (2007) 18985–18994.

[20] L. Lin, W. Lin, Y. Zhu, B. Zhao, Y. Xie, Chem. Lett. 34 (2005) 284–285.
[21] L. Bin, Y. Shu, L. Ruixing, W. Yuhua, T. Sato, J. Ceram. Soc. Jpn. (2007) 692–696.
[22] R. Asahi, T. Morikawa, T. Ohwaki, K. Aoki, Y. Taga, Science 293 (2001) 269–271.
[23] C.D. Valentin, G. Pacchioni, A. Selloni, S. Livraghi, E. Giamello, J. Phys. Chem. B 109 (2005) 11414–11419.
[24] S. Livraghi, M.R. Chierotti, E. Giamello, G. Magnacca, M.C. Paganini, G. Cappelletti, C.L. Bianchi, J. Phys. Chem. C 112 (2008) 17244–17252.
[25] Z.P. Wang, W.M. Cai, X.T. Hong, X.L. Zhao, F. Xu, C.G. Cai, Appl. Catal. B: Environ. 57 (2005) 223–231.
[26] J.L. Gole, J.D. Stout, C. Burda, Y. Lou, X. Chen, J. Phys. Chem. B 108 (2004) 1230–1240.
[27] H. Han, R.B. Bai, Ind. Eng. Chem. Res. 48 (2009) 2891–2898.
[28] T. Sugimoto, X.P. Zhou, A. Muramatsu, J. Colloid Interface Sci. 259 (2003) 53–61.
[29] Y. Murakami, T. Matsumoto, Y. Takasu, J. Phys. Chem. B 103 (1999) 1836–1840.
[30] L.S. Birks, H. Friedman, J. Appl. Phys. 17 (1946) 687–692.
[31] H. Xu, L.Z. Zhang, J. Phys. Chem. C 113 (2009) 1785–1790.
[32] M.S. Lee, S.S. Hong, M. Mohseni, J. Mol. Catal. A: Chem. 242 (2005) 135–140.
[33] X.F. Qiu, C. Burda, Chem. Phys. 339 (2007) 1–10.
[34] S. Livraghi, M.C. Paganini, E. Giamello, A. Selloni, C. Di Valentin, G. Pacchioni, J. Am. Chem. Soc. 128 (2006) 15666–15671.
[35] X.T. Zhang, K. Udagawa, Z.Y. Liu, S. Nishimoto, C.S. Xu, Y.C. Liu, H. Sakai, M. Abe, T. Murakami, A. Fujishma, J. Photochem. Photobiol. A: Chem. 202 (2009) 39–47.
[36] I.C. Kang, Q. Zhang, S. Yin, T. Sato, F. Saito, Appl. Catal. B: Environ. 84 (2008) 570–576.
[37] S. Yin, K. Ihara, M. Komatsu, Q.W. Zhang, F. Saito, T. Kyotani, T. Sato, Solid State Commun. 137 (2006) 132–137.
[38] Y. Cong, J.L. Zhang, F. Chen, M. Anpo, J. Phys. Chem. C 111 (2007) 6976–6982.
[39] M. Sathish, B. Viswanathan, R.P. Viswanath, C.S. Gopinath, Chem. Mater. 17 (2005) 6349–6353.
[40] M.Y. Xing, J.L. Zhang, F. Chen, Appl. Catal. B: Environ. 89 (2009) 563–569.
[41] H.Q. Wang, J.P. Yan, W.F. Chang, Z.M. Zhang, Catal. Commun. 10 (2009) 989–994.
[42] Z. Jiang, F. Yang, N.J. Luo, B.T.T. Chu, D.Y. Sun, H.H. Shi, T.C. Xiao, P.P. Edwards, Chem. Commun. (2008) 6372–6374.
[43] M. Bellardita, M. Addamo, A. Di Paola, L. Palmisano, A.M. Venezia, Phys. Chem. Chem. Phys. 11 (2009) 4084–4093.
[44] E. Gyorgy, A.P. del Pino, P. Serra, J.L. Morenza, Surf. Coat. Technol. 173 (2003) 265–270.
[45] S. Yin, Y. Aita, M. Komatsu, T. Sato, J. Eur. Ceram. Soc. 26 (2006) 2735–2742.
[46] S. In, A. Orlov, F. Garcia, M. Tikhov, D.S. Wright, R.M. Lambert, Chem. Commun. (2006) 4236–4238.
[47] T. Okato, T. Sakano, M. Obara, Phys. Rev. B 72 (2005).
[48] X.F. Qiu, Y.X. Zhao, C. Burda, Adv. Mater. 19 (2007) 3995–3999.
[49] H.Q. Sun, Y. Bai, H.J. Liu, W.Q. Jin, N.P. Xu, G.J. Chen, B.Q. Xu, J. Phys. Chem. C 112 (2008) 13304–13309.
[50] K.S. Yang, Y. Dai, B.B. Huang, J. Phys. Chem. C 111 (2007) 12086–12090.
[51] H. Irie, Y. Watanabe, K. Hashimoto, J. Phys. Chem. B 107 (2003) 5483–5486.